CHAPTER 4

Electrical and Ammonia Gas Sensing Properties of PQT-12 Based Organic Thin Film Transistors Fabricated by Floating-Film Transfer Method*

Contents

*Part of this work has been published as:

1. Chandan Kumar et al., "Electrical and ammonia gas sensing properties of poly(3, 3‴-dialkylquaterthiophene) based organic thin film transistors fabricated by floating-film transfer method," Organic Electronics, vol. 48, pp. 53-60, 2017.

CHAPTER 4

Electrical and Ammonia Gas Sensing Properties of PQT-12 Based Organic Thin Film Transistors Fabricated by Floating-Film Transfer Method

4.1 Introduction

It has already been discussed in Chapter-3 that PQT-12 polymer based OTFT has better ammonia gas response than PQT-12 thin film based MSM sensor presented in Chapter-2. It has also been shown that the thin film composites of CdSe QDs and PQT-12 based OTFT has better ammonia gas response than the pristine PQT-12. The literature review in Chapter-1 shows that the floating-film transfer method (FTM) provides well-oriented and self-assembled polymer films which could be better suitable for sensing applications than the conventional spin-coated polymer films [43], [147]. The FTM based polymer films are similar to the Langmuir-Blodgett films with the exception that no surface-pressure is required to be applied in the FTM technique [44], [45]. Many researchers have optimized the FTM technique for different conducting polymers [39], [46]–[48], [70]. In general, the organic devices with an FTM based polymer film is observed to have better electrical and sensing responses to gas and light over conventional spin coated polymer films [70], [147]. However, FTM based PQT-12 films have not been explored for NH_3 gas sensing applications. That is why, the present chapter reports the NH_3 gas sensing characteristics of an OTFT using the FTM based PQT-12 thin film as the active material. The performance of the proposed OTFT ammonia sensor has been compared with that of the spin-coated PQT-12 based OTFT ammonia gas sensor. The layout of the rest of this chapter is given below:

Section 4.2 discusses the experimental details for fabricating the OTFT using FTM based PQT-12 film. Section 4.3 provides some important results related to the surface and structural morphologies of the FTM and spin-coat based PQT-12 films. The electrical and ammonia gas sensing characteristics of the FTM based OTFT have been compared to those of spin-coated PQT-12 based OTFT. Finally, Section 4.4 concludes the major observations and finding of this Chapter.

4.2 Experimental Details

In this section, PQT-12 thin film deposition and OTFT fabrication steps using FTM and spin-coat techniques are presented.

4.2.1 Thin Film Deposition

Heavily doped p-type silicon <100> (resistivity 0.01-0.02 ohm-cm) is used as the substrate and bottom gate for the OTFT sensor under consideration. The silicon substrates are first cleaned by standard wet cleaning procedure and vacuum dried before oxidation [165]. Thereafter, the cleaned silicon substrates are kept in a cylindrical muffle furnace for growing a 100 nm SiO_2 layer by the dry oxidation method. Self-assembled monolayer (SAM) treatment of the SiO_2 layer is performed by spin coating 1 mM OTS in toluene at 3000 rpm for 110 s for the surface modification of SiO_2 layer [172], [173]. The SiO_2 layer is then dried in a vacuum oven at 150°C for 60 min.

For the deposition of PQT-12 FTM film, 5 mg PQT-12 is dissolved in 1 ml chloroform and the solution is warmed with stir for 5 min. The liquid surface is made in a petri dish by a hydrophilic solution of ethylene glycol (EG) and glycerol (G) in the ratio of 1:1 [112]. After 5 min, 15 µl of the PQT-12 solution is dropped at the centre of the liquid surface. The PQT-12 solution is dispersed on the liquid surface to form a self-assembled floating film. Thereafter, the floated film is stamped on the OTS-treated

substrate shown in Figure 4.1 and washed with methanol to remove any residue of the liquid surface. In order to compare the surface morphologies of the FTM based PQT-12 film with the conventional spin-coated PQT-12 film, we have used 1 mg/ml solution of the PQT-12 for depositing a film on the OTS-treated Si/SiO_2 substrates by using spin coating method.

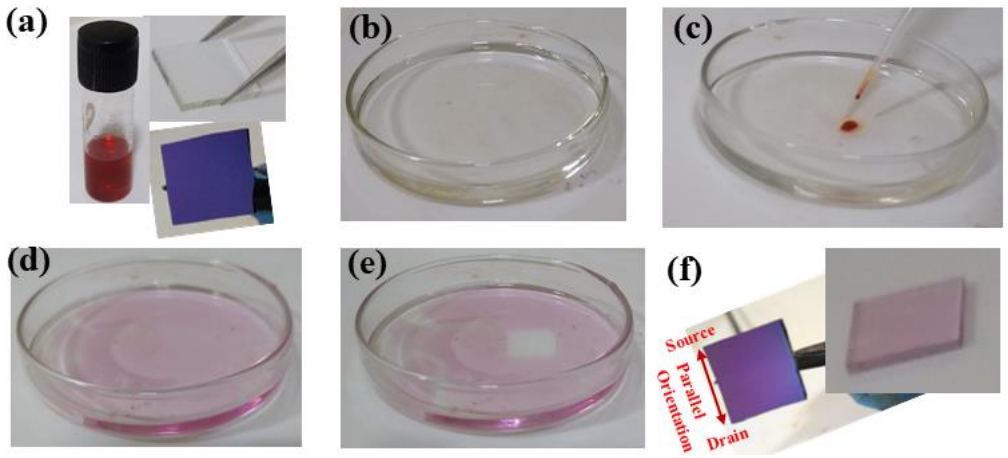

Figure 4.1: Camera image of the FTM steps: (a) PQT-12 solution in chloroform and substrates (glass and Si/SiO_2), (b) Hydrophilic solution of EG and G (1:1), (c) Drop of PQT-12 on liquid surface, (d) PQT-12 film on liquid surface, (e) PQT-12 film on liquid surface after stamping on solid sample, and (f) FTM coated PQT-12 film on glass and Si/SiO_2 substrates.

4.2.2 Fabrication of Organic Thin Film Transistor

It may be mentioned that the thickness of PQT-12 film plays an important role with the charge transport phenomenon between source and drain of the OTFT. The drain current of the OTFT sensor is normally increased with increased PQT-12 film thickness whereas a reverse trend is observed for the response of the sensor [79], [80]. Thus, the thickness for both the FTM and spin coated PQT-12 films has been optimized to ~20 nm for enhanced gas response with a significant drain current of the OTFT sensors under study [70]. The PQT-12 film is dried at 110°C for 60 min in the flow of nitrogen gas. We have fabricated the parallel OTFT structure [28], [39] on the Si/SiO_2 substrate as shown in Figure 4.1 (f) for achieving the maximum possible carrier mobility in the

channel. To form the source and drain contacts, thin interfacial hole transport layers (~6 nm) of MoO_3 is first deposited on the PQT-12 film and then silver of 60 nm is deposited on MoO_3 to form the source and drain contacts. Note that the interfacial layer of MoO_3 is used to enhance the effective work function of the silver electrodes [174] as shown in the energy band diagram of Figure 4.2. The MoO_3 and silver layers have been deposited by thermal vacuum deposition using a shadow mask technique for channel length and channel width of 30 µm and 1 mm, respectively as shown in Figure 4.3. A 60 nm thin silver layer is also deposited on the backside of the Si substrate to work as the gate contact of OTFT sensor structure. The thermal deposition of Ag and MoO_3 is performed at high vacuum (~3×10^{-6} mbar) at the rate of 0.5 Å/s.

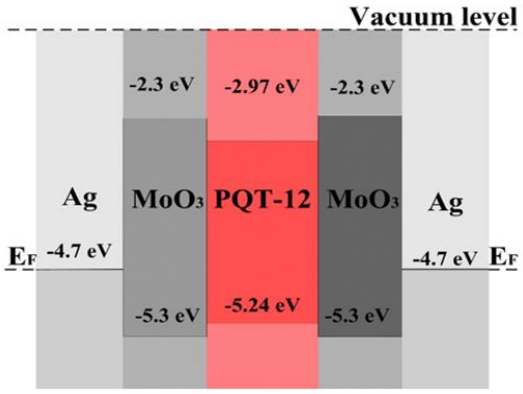

Figure 4.2: Energy band diagram between PQT-12 and source/drain of the OTFT.

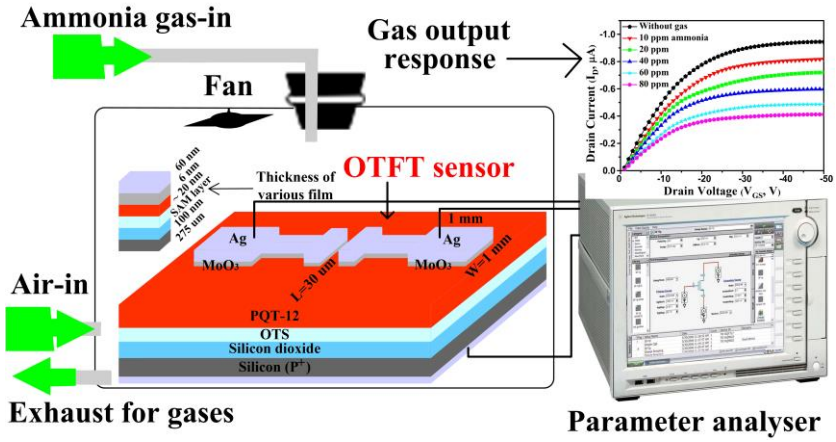

Figure 4.3: Device structure of the organic thin film transistor along with a block diagram of gas sensing setup.

4.3 Results and Discussion

In this section, the PQT-12 thin film and electrical as well as ammonia gas sensing characterization are discussed.

4.3.1 Thin Film Characterization

The alignment of polymer chains in the FTM coated PQT-12 film can be observed in the AFM topography shown in Figure 4.4 (a) while no regular alignment of the polymer chains is observed in the AFM topography of the spin coated PQT-12 film shown in Fig. 4.4 (b). The respective values of the average roughness, root mean square roughness and peak-to-peak spacing estimated by using the Nova PX software are 1.3 nm, 1.6 nm and 11.5 nm for the FTM film and 0.8 nm, 1.0 nm and 10.6 nm for the spin-coated film. Although both the films have nano-level roughness, the higher roughness of the FTM based PQT-12 films is believed to provide better gas sensing performance than the spin-coated PQT-12 films.

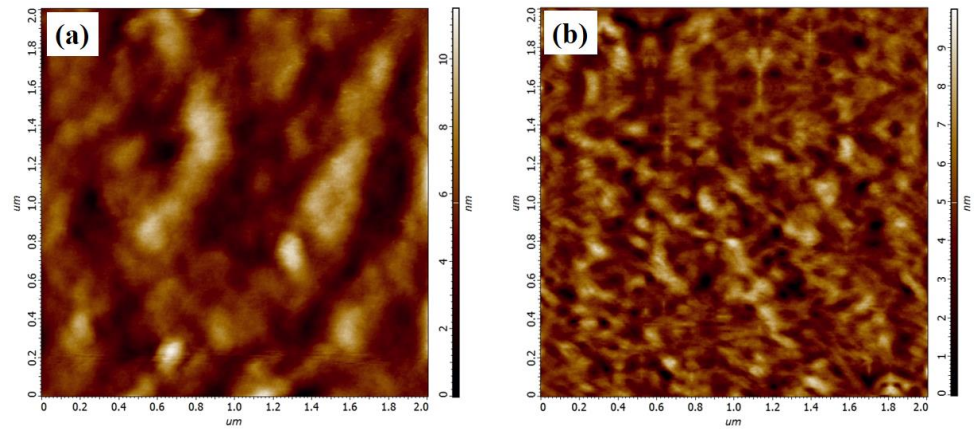

Figure 4.4: AFM topography of (a) FTM film and (b) Spin-coated film on OTS treated Si/SiO_2 substrate.

4.3.2 Electrical Characterization

The electrical characterization of the OTFT sensor has been carried out under ambient condition (room temperature, 23°C and 56% humidity). The measured output characteristics of the as-fabricated FTM based PQT-12 OTFT have been plotted for different applied gate voltage (V_{GS}) in Figure 4.5. To compare the performances of the

FTM and spin coated PQT-12 films, the output characteristics of the spin-coated PQT-12 based OTFT sensor have been plotted as shown in Figure 4.6. For a fixed gate bias voltage, the higher drain current in the FTM based OTFT as compared to its corresponding value for the spin-coated OTFT device implies a better PQT-12 film quality in the former device than the later device [43]. We have also compared the transfer characteristics (I_D vs. V_{GS}) of both the FTM and spin coated OTFTs as shown in Figure 4.7 for an applied drain voltage (V_{DS}) of -50 V to extract the device performance parameters such as the field effect mobility (μ), the threshold voltage (V_{th}), on/off current ratio and subthreshold swing (SS) for both the FTM and spin-coated OTFT sensors.

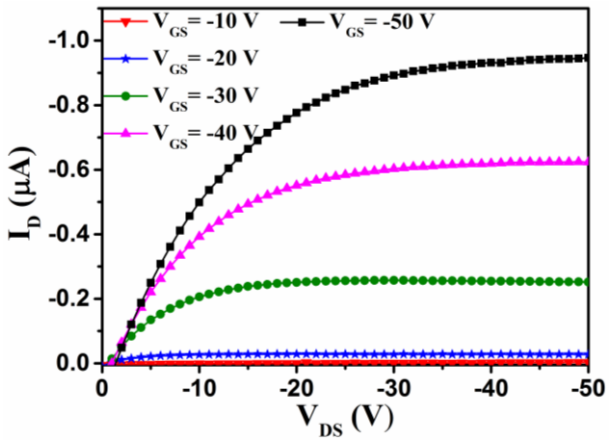

Figure 4.5: Output characteristics of as-fabricated FTM coated OTFT sensor.

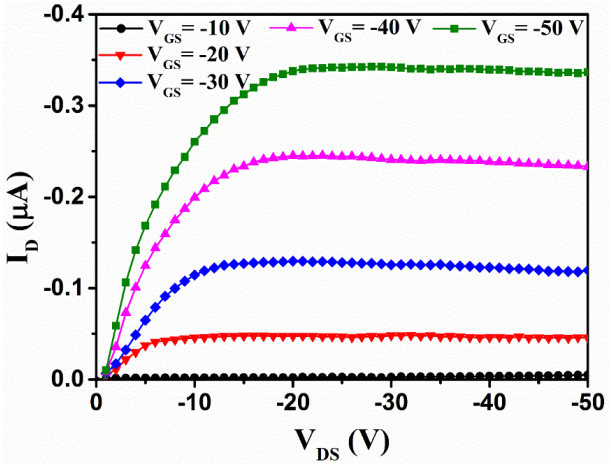

Figure 4.6: Output characteristics of the spin-coated OTFT sensor.

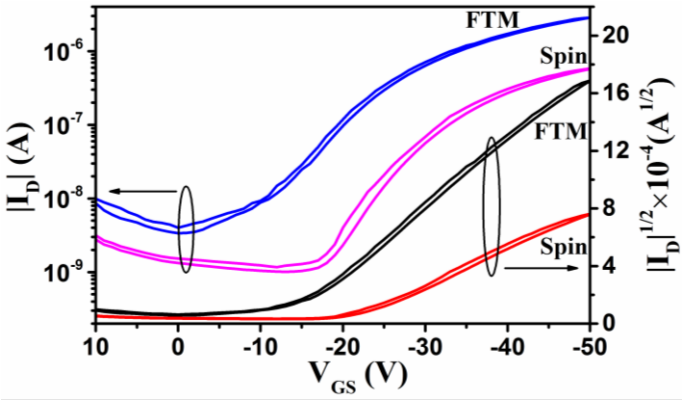

Figure 4.7: Transfer characteristics of as-fabricated OTFT sensor based on FTM and spin-coating PQT-12 film.

Since the FETs are normally operated in the saturation region, we have extracted the parameters by modeling the transfer characteristics (I_D vs. V_{GS}) in the saturation region of the OTFT as [168]:

$$I_D = \frac{W}{2L}\mu C_i \left(V_{GS} - V_{th}\right)^2 \tag{4.1}$$

We thus write,

$$\sqrt{I_D} = \sqrt{\frac{W}{2L}\mu C_i}\left(V_{GS} - V_{th}\right) = P\left(V_{GS} - Q\right) \tag{4.2}$$

which gives,

$$V_{GS} = \frac{1}{P}\sqrt{I_D} + Q \tag{4.3}$$

where, I_D is the drain current, L and W are the channel length and width, respectively, C_i is the capacitance per unit area of the SiO_2 layer, and P is the slope of the line $\sqrt{I_D}$ vs. V_{GS} characteristics, given by

$$P = \frac{\partial\sqrt{I_D}}{\partial V_{GS}} = \sqrt{\frac{WC_i}{2L}\mu} \tag{4.4}$$

The threshold voltage has been estimated from the extrapolation of the line $\sqrt{I_D}$ vs. V_{GS}. The on/off current ratio (I_{ON}/I_{OFF}) has been computed from the transfer

characteristic by using $I_{ON} = \left| I_D \left(V_{GS,max}, V_{DS,max} \right) \right|$ and $I_{OFF} = min \left| I_D \left(V_{DS,max} \right) \right|$, where $V_{GS,max}$ is the maximum applied gate to source voltage and $V_{DS,max}$ is the maximum applied drain to source voltage. The subthreshold swing of the OTFT has been extrapolated from the logarithmic plot of I_D vs. V_{GS} as $SS = \max \left| \left(\partial \log_{10} \left| I_D \left(V_{DS,\max} \right) \right| / \partial V_{GS} \right)^{-1} \right|$. The field effect mobility, threshold voltage, on/off current ratio, and the subthreshold swing of the FTM and spin coated OTFTs under study have been summarized in Table 4.1. The higher mobility and lower threshold voltage in the FTM based OTFT are attributed to self-assembled and better oriented PQT-12 film than the spin-coated films [43], [147], which enhance the charge transport in the channel. These device performance parameters of the OTFT are in good agreement with other reported results in the literature [34], [74], [108].

Table 4.1: Comparison of performance parameters of FTM and spin-coated PQT-12 based OTFT.

OTFT parameters	**FTM**	**Spin**
Mobility ($\times 10^{-3}$ cm^2/V-s)	8.77	2.96
Threshold voltage (V)	-13.9	-22.3
on/off current ratio	843	563
Sub-threshold swing (V/dec)	8.5	5.6

4.3.3 Gas Sensing Characterization

The measured drain current versus drain voltage characteristics of the FTM based OTFT sensor has been shown in Figure 4.8 for different NH_3 gas concentrations varying from 10 ppm to 80 ppm. When the device is exposed to NH_3 gas, NH_3 gas molecules are adsorbed in the PQT-12 film which reduces the charge carriers (holes) by enhancing the trap density in the channel [175]. This increases the threshold voltage of the OTFT since more gate voltage is required to compensate the decrease in the charge carriers in

the channel due to NH_3 adsorption. As a consequence, the sensor performance parameters such as field effect mobility and on/off current ratio are decreased whereas the threshold voltage is increased with the increased NH_3 gas concentration. The transfer characteristics at V_{DS} = -50 V for FTM coated and spin coated OTFT have been plotted for 80 ppm of NH_3 gas as shown in Figure 4.9. The field effect mobility, threshold voltage, and on/off ratio are determined as 5.72×10^{-3} cm^2/V-s, -17.7 V, and 545, respectively at 80 ppm of NH_3 gas for FTM coated OTFT sensor. The values of field effect mobility and the threshold voltage at various concentration of NH_3 gas for FTM coated sensor have been calculated and plotted in Figure 4.10.

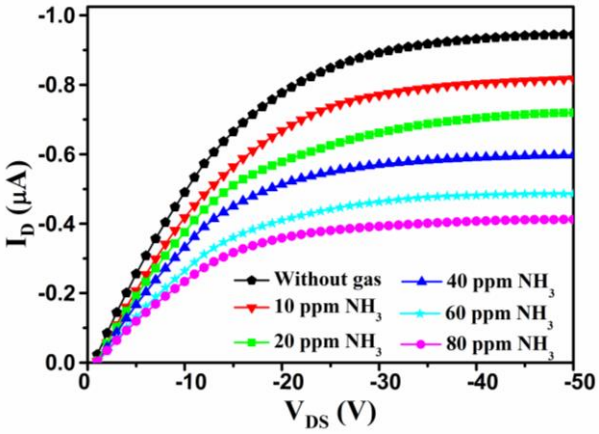

Figure 4.8: Output characteristics of FTM coated OTFT for different NH_3 gas concentrations measured at V_{GS} = -50 V.

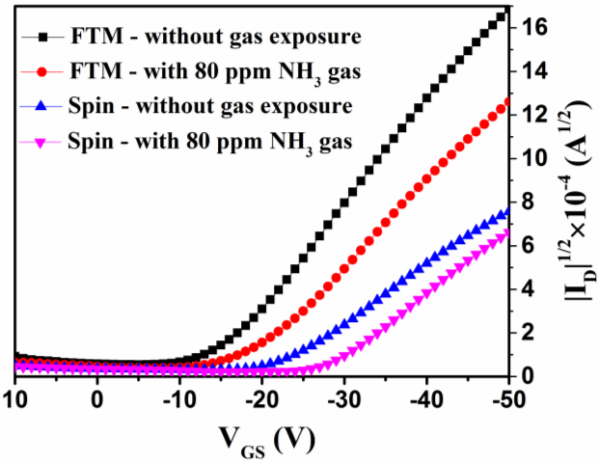

Figure 4.9: Transfer characteristic of the as-fabricated sensor using FTM and spin coating: without gas exposer and with 80 ppm NH_3 gas exposer.

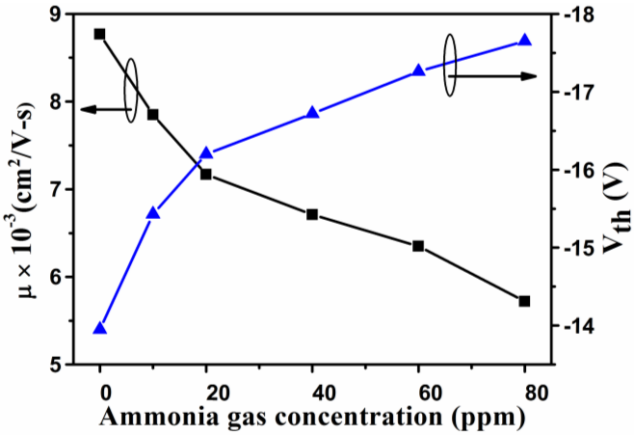

Figure 4.10: Variation in field effect mobility and the threshold voltage of FTM coated OTFT at various concentration of NH_3 gas.

The hysteresis observed in the transfer characteristics shown in Figure 4.7 is attributed to the trap charges [34], [176]. The trap charge (Q_{trap}) in the dielectric-polymer interface may be computed by using the device parameters extracted from the transfer characteristic as [175]:

$$Q_{trap} = \Delta V_{th} C_i \tag{4.5}$$

Thus, the trap charge density (N) is given by

$$N = \frac{Q_{trap}}{q} \tag{4.6}$$

where q is the charge of the electron. The trap carrier density is observed to be increased from $1.47\times10^{12}/cm^2$ to $1.87\times10^{12}/cm^2$ when the NH_3 concentration in the gas characterization chamber is increased from zero to 80 ppm.

The gas response (S) of OTFT sensor under study is defined as the ratio of change in drain current ($I_{D,air} - I_{D,gas}$) on gas exposure to the initial drain current ($I_{D,air}$) in the air [177].

$$S = \frac{I_{D,air} - I_{D,gas}}{I_{D,air}} \times 100\% \tag{4.7}$$

The gas responses of the FTM based OTFT sensor for various concentrations of NH_3 gas varying from 10 ppm to 80 ppm have been calculated and plotted in Figure 4.11. The transient characteristics (i.e. time versus response curve) shown in Figure 4.11 has been measured for $V_{GS} = V_{DS} = -50$ V.

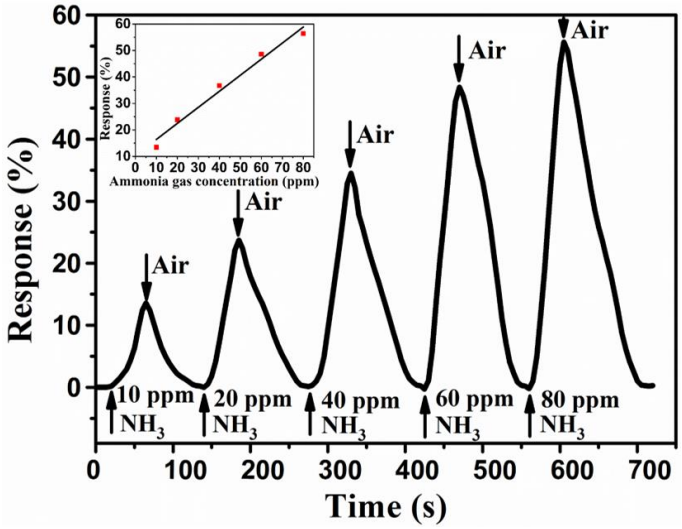

Figure 4.11: Transient response of FTM coated OTFT sensor for various concentration of a NH_3 gas. The response vs. ammonia gas concentration curve with linearly fitted is in the inset.

The gas response is increased with the increased concentration of NH_3 gas and then it is slightly saturated for higher concentration. The NH_3 gas molecules are absorbed in the PQT-12 film thereby resulting in a charge transfer from NH_3 molecules to the PQT-12 film as in P3HT film [72]. The NH_3 gas molecules create trap charges in the PQT-12 film. This reduces the hole carrier concentration in the channel, which, in turn, reduces drain current as discussed earlier. We have measured the gas response of 56.4% at 80 ppm of NH_3 gas with response time (T_{res}) and recovery time (T_{rec}) of ~45 s and ~85 s, respectively in FTM coated OTFT sensor. The performance parameters of the FTM coated OTFT ammonia sensor at various concentration of ammonia gas have been summarized in Table 4.2.

Table 4.2: The FTM coated OTFT sensor performance parameters for ammonia gas.

Ammonia (ppm)	**Mobility ($\times 10^{-3}$ cm^2/V-s)**	**Threshold Voltage (V)**	**On/off Ratio**	**Trap density ($\times 10^{12}$/cm^2)**	**Response (%)**
0	8.77	-13.9	843	1.47	0
10	7.85	-15.4	729	1.62	13.5
20	7.17	-16.2	660	1.71	23.8
40	6.71	-16.7	598	1.76	36.7
60	6.35	-17.3	571	1.82	48.6
80	5.72	-17.7	545	1.87	56.4

The responses for various ammonia gas concentration have been plotted with respect to ammonia gas concentration and linearly fitted as shown in the inset of Figure 4.11. This plot is called as sensitivity plot, and its slope is the sensitivity per ppm. Further, from noise theory, any signal would be real only if the signal-to-noise ratio ≥ 3, therefore the detection limit (DL) for the OTFT ammonia sensor under study can be calculated from the following equation [162]:

$$DL(ppm) = 3\frac{rmsd}{sensitivity} \tag{4.8}$$

Using the values of rmsd = 8.16×10^{-4} and sensitivity = 6.06×10^{-3} ppm^{-1} in Equation (4.8), the detection limit of the as-fabricated PQT-12 based OTFT sensor using FTM under consideration is determined as 404 ppb. The sensing parameters of the OTFT sensor using FTM and spin-coating have been compared and listed in Table 4.3. The performance parameters of our OTFT sensor using FTM and spin coating are in good agreement with the reported results for other organic material based sensors [122], [130], [124], [170]. The comparative results of the other reported NH_3 gas sensors have been sum-up and listed in Table 4.4.

Table 4.3: Comparative list of sensing parameters of OTFT using FTM and spin-coating.

Sensing parameters of OTFT	**FTM**	**Spin**
Response for 80 ppm ammonia gas (%)	~56.4	~23.9
Response time for 80 ppm ammonia gas (s)	~ 45	~42
Recovery time for 80 ppm ammonia gas (s)	~85	~86
Detection limit (ppb)	404	814

Table 4.4: Comparative list of reported sensors for ammonia gas.

References	**S (%)**	**T_{res}**	**T_{rec}**	**NH_3 (ppm)**	**Sensing material**	**Film deposition technique**	**Device structure**
This work	~56.4	~ 45 s	~85 s	80	PQT-12	FTM	Transistor
Han et al. [122]	51.1	-	-	50	P3HT/Polystyrene	Spin coat	Transistor
Chen et al. [130]	19 27	~3.5 min ~3 min	~12 min ~9 min	100	P3HT P3HT/PC61BM	Airbrush-deposition	Transistor
Xie et al. [124]	~0.8	5 min	5 min	100	P3HT/RGO	Airbrush-deposition	Transistor
Yu et al. [170]	14.8	~5 min	~50 min	100	Pentacene	Thermal evaporation	Transistor
Besar et al. [68]	~31.4	5 min	-	1.5	PQT-12	Drop cast	Transistor
Dai et al. [33]	~41	200 s	800 s	0.5	PQT-12	Spin coat	Diode
Vieira et al. [67]	Very low	20 s	-	100	PQT-12	Drop cast	MSM

The ammonia gas sensing mechanism through the PQT-12 film in OTFTs can be explained as a chemical interaction between both, where the NH_3 gas molecules cause de-doping in the polymer chain as in P3HT molecule [72]. Under normal operating condition without NH_3 gas exposure, the gate of the as-fabricated OTFT sensor is applied with a negative voltage. Due to this negative gate voltage, the positive charges are accumulated at the polymer-dielectric interface and form a conducting channel at the interface. When the OTFT sensor is exposed to the various concentration of NH_3 gas,

the lone pair of electron in NH_3 gas get interacted with PQT-12 and reduce the net positive charges (holes) in the polymer as shown in Figure 4.12. This reduction in hole concentration decreases the drain current of the as-fabricated sensor, as a result, the OTFT sensor parameters viz. field effect mobility, threshold voltage, on/off ratio, etc. get changed. The interaction of electron lone pair with the positive charges in PQT-12 starts altering the molecular structure. When the air is injected into the gas chamber during recovery, the a NH_3 gas gets discarded with the electron lone pair from the PQT-12 chain and the polymer regains its stable molecular structure.

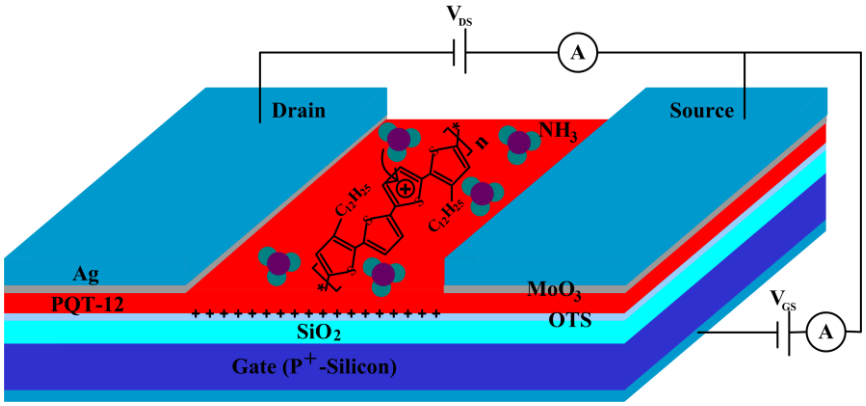

Figure 4.12: Ammonia gas interaction mechanism in the as-fabricated OTFT sensor.

4.4 Conclusion

The PQT-12 polymer based OTFT ammonia gas sensor is fabricated on p-type silicon substrate by the floating-film transfer method (FTM). The electrical and ammonia gas sensing characteristics of the FTM based OTFT sensor have been compared with those of spin-coated OTFT ammonia sensors. The values of the field effect mobility, threshold voltage, on/off current ratio and subthreshold swing of the OTFT estimated from the transfer characteristics of the device are 8.77×10^{-3} cm^2/V-s, -13.9 V, 843 and 8.5 V/dec, respectively for FTM coated devices whereas 2.96×10^{-3} cm^2/V-s, -22.3 V, 563 and 5.6 V/dec, respectively for spin coated devices. The *IV* characteristics measured under different concentrations of ammonia gas varying from

10 ppm to 80 ppm show a decrease in the drain current with the increased ammonia concentration due to charge trapping of the channel carriers into the absorbed ammonia molecules in the film. Ammonia gas response of 56.4%, response time of ~45 s, recovery time of ~85 s, and detection limit of 404 ppb at 80 ppm of ammonia gas have been achieved for FTM coated devices. The field effect mobility, threshold voltage and on/off current ratio of the OTFT sensor are significantly changed when the device is exposed to the ammonia gas. All the performance parameters of our FTM based OTFT ammonia sensor are superior to spin-coated OTFT sensors. The results are in good agreement with the other reported results for ammonia gas sensors using different polymers.